

Supporting Information

Understanding Nonlinear Optical Phenomena in N-Pyrimidinyl Stilbazolium Crystals via a Self-Consistent Electrostatic Embedding – DFT Approach

Renato Medeiros^{a,b}, Leandro R. Franco^c, Francisco A.P. Osório^a, Clodoaldo Valverde^{b,d}, Marcos A. Castro^a and Tertius L. Fonseca^{a,*}

^aInstituto de Física, Universidade Federal de Goiás, Goiânia-GO, 74690-900, Brazil.

^bCampus de Ciências Exatas e Tecnológicas, Universidade Estadual de Goiás, Anápolis-GO, 75001-970, Brazil

^cDepartment of Engineering and Physics, Karlstad University, 65188 Karlstad, Sweden.

^dUniversidade Paulista, Goiânia-GO, 74845-090, Brazil.

Table S1. CAM-B3LYP results for the static linear and nonlinear optical properties of the OPR-based crystals obtained with the 6-311++G(d,p) and 6-311G(d,p) basis set.

| Basis set | OPR-CBS (isolated) | OPR-CBS (embedded) | OPR-T (isolated) | OPR-T (embedded) | OPR-VBS (isolated) | OPR-VBS (embedded) |
|--|-----------------------|-----------------------|---------------------|---------------------|-----------------------|-----------------------|
| $\langle \alpha \rangle$ (in 10^{-24} esu) | | | | | | |
| 6-311++G(d,p) | 56.48 | 58.75 | 55.21 | 56.23 | 58.24 | 58.94 |
| 6-311G(d,p) | 52.73 | 54.76 | 51.74 | 52.56 | 54.45 | 54.93 |
| β_{tot} (in 10^{-30} esu) | | | | | | |
| 6-311++G(d,p) | 179.45 | 233.12 | 170.19 | 196.63 | 180.82 | 211.96 |
| 6-311G(d,p) | 175.18 | 223.71 | 166.31 | 190.25 | 177.45 | 205.57 |
| β_{zzz} (in 10^{-30} esu) | | | | | | |
| 6-311++G(d,p) | 44.24 | 19.56 | 25.01 | 8.45 | 36.74 | 13.58 |
| 6-311G(d,p) | 41.63 | 16.48 | 23.55 | 6.94 | 34.49 | 11.53 |
| β_{yyy} (in 10^{-30} esu) | | | | | | |
| 6-311++G(d,p) | -82.48 | -166.97 | -103.54 | -165.40 | -91.43 | -156.83 |
| 6-311G(d,p) | -82.75 | -163.46 | -103.48 | -162.25 | -92.82 | -154.77 |
| $\langle \gamma_{\parallel} \rangle$ (in 10^{-36} esu) | | | | | | |
| 6-311++G(d,p) | 294.42 | 343.14 | 293.75 | 316.57 | 332.05 | 367.26 |
| 6-311G(d,p) | 261.23 | 291.54 | 263.06 | 275.92 | 295.18 | 322.18 |

Table S2. CAM-B3LYP results for vector components of ground-state dipole moment ($\vec{\mu}_{gg}$), excited-state dipole moment ($\vec{\mu}_{ee}$) and transition dipole moment ($\vec{\mu}_{ge}$) of the OPR crystals. All values are given in D.

| Crystal | $\mu_{gg,x}$ | $\mu_{gg,y}$ | $\mu_{gg,z}$ | $\mu_{ee,x}$ | $\mu_{ee,y}$ | $\mu_{ee,z}$ | $\mu_{ge,x}$ | $\mu_{ge,y}$ | $\mu_{ge,z}$ |
|---------|--------------|--------------|--------------|--------------|--------------|--------------|--------------|--------------|--------------|
| OPR-CBS | 11.531 | -2.812 | 14.610 | 8.418 | 5.200 | 13.155 | -3.349 | 10.016 | -0.819 |
| OPR-T | 11.531 | -2.812 | 14.610 | 8.418 | 5.200 | 13.155 | -2.637 | 9.938 | -0.807 |
| OPR-VBS | 10.918 | -1.515 | 14.142 | 4.554 | 6.408 | 8.893 | -3.188 | 8.312 | -0.564 |

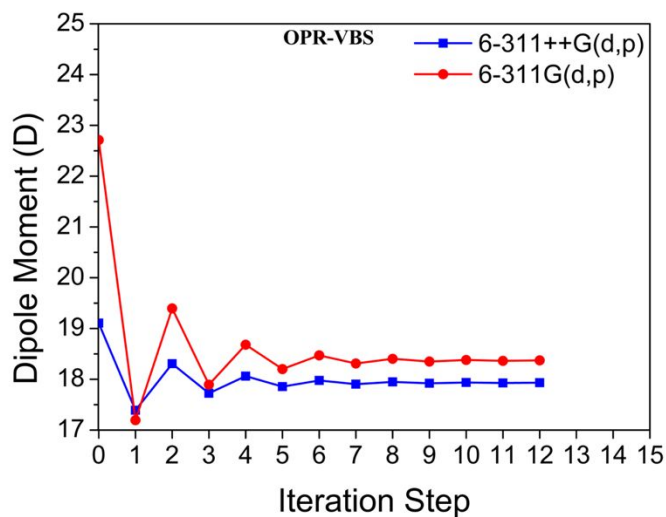
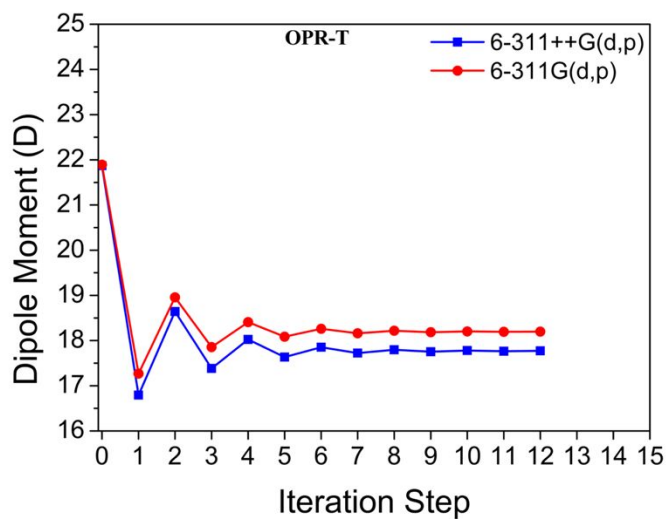
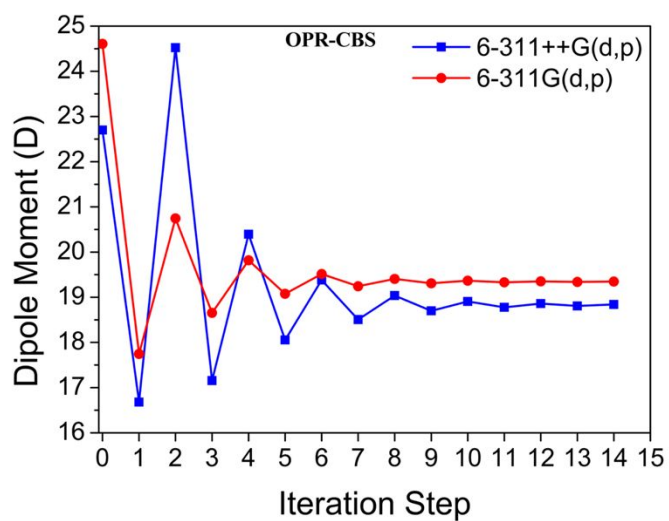


Figure S1. Convergence of dipole moment of the OPR-based crystals as function of the iterative procedure.

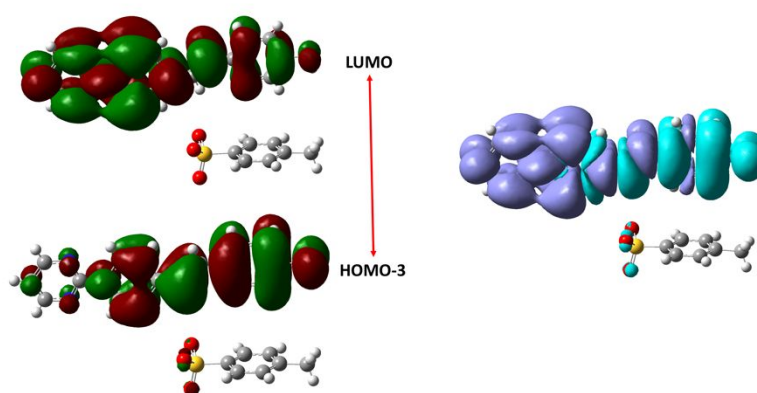
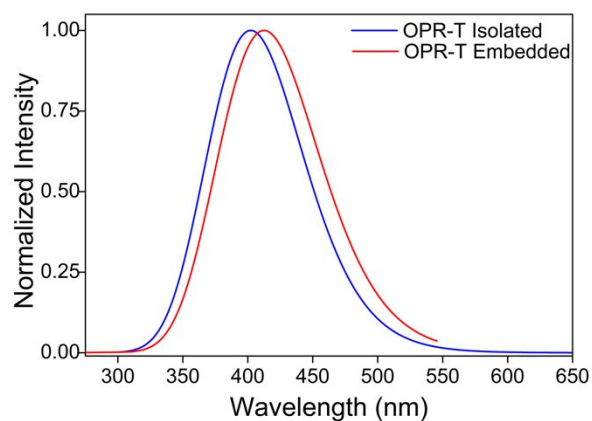


Figure S2. Theoretical UV–Vis absorption spectra of unit cell of OPR-T crystal. Gaussian convolution with full width at half maximum (FWHM) of 0.3 eV. Frontier orbitals involved in the dominant transition and change in electron density. The aqua blue (purple) color indicates the region where the electrons are coming (arriving).

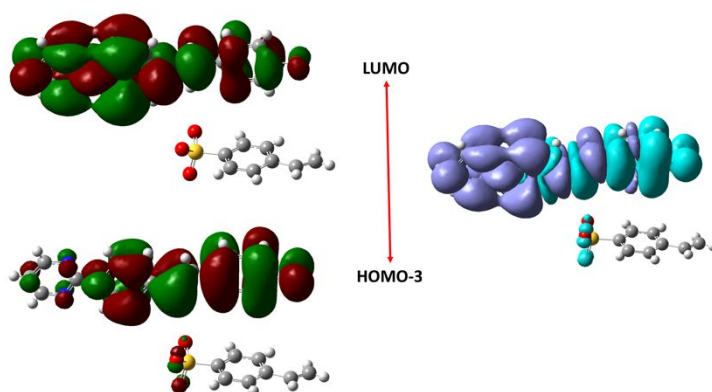
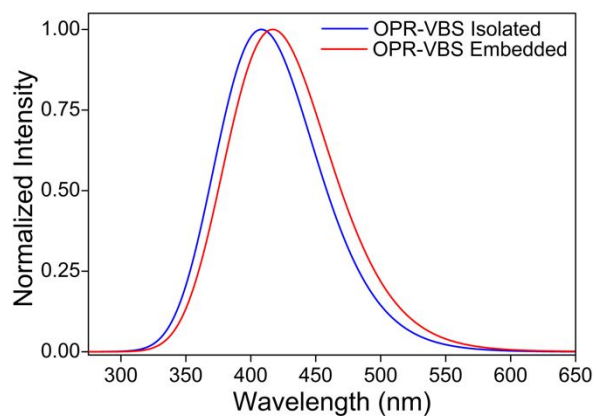


Figure S3. Theoretical UV–Vis absorption spectra of unit cell of OPR-VBS crystal. Gaussian convolution with full width at half maximum (FWHM) of 0.3 eV. Frontier orbitals involved in the dominant transition and change in electron density. The aqua blue (purple) color indicates the region where the electrons are coming (arriving).